



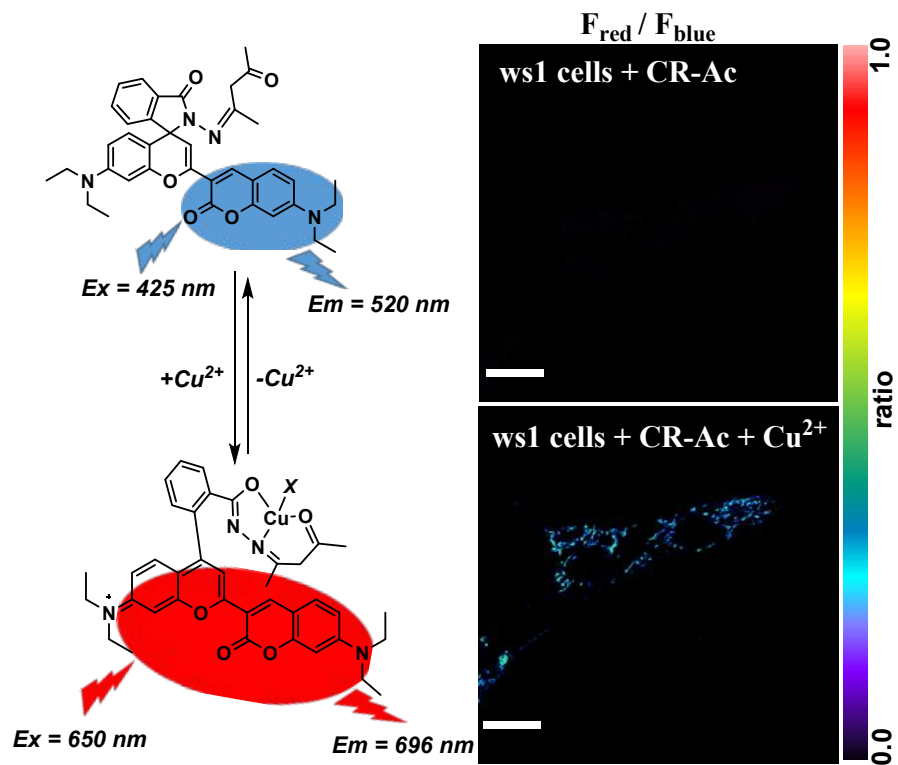
ChemComm

**A novel near-infrared ratiometric fluorescent probe capable of copper(II) ion determination in living cells**

Journal:	<i>ChemComm</i>
Manuscript ID	CC-COM-02-2020-001481.R2
Article Type:	Communication

SCHOLARONE™  
Manuscripts

A novel NIR ratiometric fluorescent probe has been developed for monitoring the dynamic changes of subcellular  $\text{Cu}^{2+}$  and quantifying its concentration at nanomolar level in live-cells.



## COMMUNICATION

## A novel near-infrared turn-on and ratiometric fluorescent probe capable of copper(II) ion determination in living cells

Ziya Aydin,<sup>\*a,b</sup> Bing Yan,<sup>c</sup> Yibin Wei,<sup>c</sup> and Maolin Guo<sup>\*b,c</sup>

Received 00th January 20xx,

Accepted 00th January 20xx

DOI: 10.1039/x0xx00000x

**A near-infrared ratiometric fluorescent probe CR-Ac based on a coumarin-benzopyrylium platform has been developed for selective detection of Cu<sup>2+</sup>. Cell imaging data revealed the capabilities of CR-Ac in monitoring the dynamic changes of subcellular Cu<sup>2+</sup> and quantification of Cu<sup>2+</sup> levels in live cells.**

### Introduction

It is well known that copper is one of the most abundant transition metals in living systems, third after iron and zinc, and a crucial micronutrient for animals and plants<sup>1</sup>. Copper (Cu<sup>+</sup> and Cu<sup>2+</sup>) functions as a key factor in many physiological processes such as signal transduction, redox reactions, the central nervous system, and energy generation<sup>1</sup>. On the other hand, it is highly toxic to living systems under unhealthy levels<sup>1</sup>. The toxicity of copper has been associated with various diseases, including Menkes and Wilson diseases, Alzheimer's and Parkinson's diseases<sup>2</sup>. Moreover, enormous quantity of copper pollution was generated to our living environment due to its widely usage in industrial sectors<sup>3</sup>. It is thus important to develop effective detection methods to efficiently evaluate Cu<sup>2+</sup> levels in environments and biological systems.

Over the past few decades, optical imaging and small molecule fluorescent probes have gained growing interest in detecting metal ions in living systems<sup>4</sup>. Probes for both Cu<sup>+</sup> and Cu<sup>2+</sup> have been reported<sup>1e,5</sup> but developing Cu<sup>2+</sup>-probes is more challenging due to its paramagnetic quenching nature and selectivity issues<sup>5</sup>. It is thus most of the current Cu<sup>2+</sup>-probes are limited to "turn-off" type, providing useful information but suffering from poor sensitivity, or interference from other metal ions<sup>6</sup>. Recently, "turn-on" copper sensors have been reported but most of them require excitation using short-wavelength UV-vis light (350–500 nm) and emit lights in the visible range<sup>5,6</sup>. Near-infrared (NIR) probes are highly desirable due to better tissue penetration, less photo damage, minimum fluorescence background, and less light scattering<sup>5</sup>. Several interesting NIR probes have

recently been reported for Cu<sup>2+</sup> imaging<sup>5,7</sup>. These sensors offer effective tools for Cu<sup>2+</sup> detection in living systems, however, quantitative measurement of free copper ion concentration in live-cells is still very challenging<sup>5</sup>. A carbonic anhydrase-dye conjugation has recently been applied for quantification of free Cu<sup>2+</sup> levels in cytoplasm via fluorescence lifetime imaging microscopy<sup>5c</sup>. However, the cytoplasm localization of the conjugate limits its ability in Cu<sup>2+</sup> detecting in cellular organelles where most of the free Cu<sup>2+</sup> are located<sup>1</sup>. Ratiometric probes may provide better tools for quantification as the ratio between two intensities can be used to measure analyte concentration and they also provide built-in correction for environmental effects. So far, only a few ratiometric probes<sup>5,8</sup> have been reported for Cu<sup>2+</sup> and only one (ACCu2)<sup>9</sup> has achieved quantification of Cu<sup>2+</sup> concentration in live cells or tissues. However, the ACCu2 probe is a turn-off type with emission in the visible region, requiring two-photon excitation and the fluorescent ratio of the ACCu2-copper complex is sensitive to pH in physiological pH range<sup>9</sup>, impeding its broad application in biological settings. Herein, we report a new turn-on NIR ratiometric fluorescent probe that overcomes the pH and two-photon issues and is capable of quantifying Cu<sup>2+</sup> concentration in live cells in real time.

Spirocyclization of xanthene dyes has become a powerful technique for developing fluorescent probes<sup>10</sup>. Recently, this unique fluorescence switching mechanism has been extended to near-infrared dyes with a coumarin-benzopyrylium platform which displays coumarin emission even in its spirocyclic closing form<sup>10</sup>. This enables the dye to exhibit visible and near-infrared emissions in its spirocyclic ring-closing and opening forms, respectively. Taking this advantage, we designed the NIR fluorescent probe CR-Ac for turn-on and ratiometric sensing of Cu<sup>2+</sup> by employing the coumarin-benzopyrylium platform as the dye scaffold and a group consisting of O/N/O receptor moiety for Cu<sup>2+</sup>. The probe, CR-Ac, was synthesized via a 4-step procedure as outlined in Scheme 1 and detailed in supporting information, with an overall yield of 34%.

We first evaluated the spectroscopic properties of CR-Ac and its interactions with various metal ions. The yellow compound CR-Ac (20 μM) in ACN/MOPS buffer (10 mM, pH 7.04, v/v 1:1) displays a maximum absorption at 424 nm (corresponding to the coumarin moiety) and almost no absorption above 500 nm, indicating that CR-Ac was dominantly in the spirocyclic form<sup>10</sup>. The metal ions such as Ni<sup>2+</sup>, Mn<sup>2+</sup>, Hg<sup>2+</sup>, Na<sup>+</sup>, Ca<sup>2+</sup>, Zn<sup>2+</sup>, Ag<sup>+</sup>, Mg<sup>2+</sup>, Pb<sup>2+</sup>, K<sup>+</sup>, Fe<sup>3+</sup>, Co<sup>2+</sup>, Fe<sup>2+</sup>, Cu<sup>+</sup> and Cr<sup>3+</sup> gave little response

<sup>a</sup> Vocational School of Technical Sciences, Karamanoğlu Mehmetbey University, 70100 Karaman, Turkey, email: ziyaaydin@kmu.edu.tr

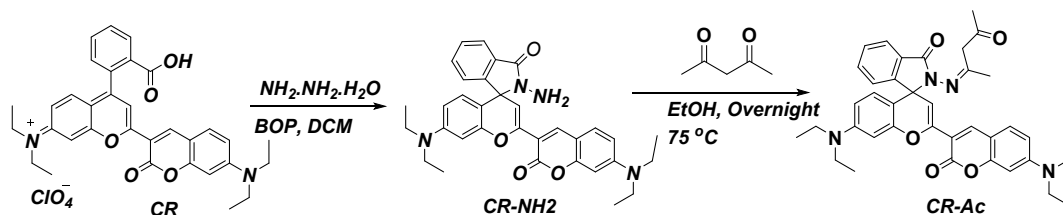
<sup>b</sup> Department of Chemistry, University of Massachusetts Amherst, 710 North Pleasant Street, Amherst, MA 01003 (USA). Email: mguo@umassd.edu

<sup>c</sup> Department of Chemistry and Biochemistry, University of Massachusetts Dartmouth, 285 Old Westport Road, Dartmouth, MA 2747 (USA).

Electronic Supplementary Information (ESI) available: [details of any supplementary information available should be included here]. See DOI: 10.1039/x0xx00000x

to CR-Ac (Figure 1a). In contrast, with increasing in  $\text{Cu}^{2+}$  concentration, the absorbance at 424 nm ( $\epsilon = 5.1 \times 10^4 \text{ M}^{-1} \text{ cm}^{-1}$ , CR-Ac only) decreased, while the absorbance at 650 nm ( $\epsilon = 2.52 \times 10^4 \text{ M}^{-1} \text{ cm}^{-1}$ , CR-Ac: $\text{Cu}^{2+}$ , 1:1) increased concomitantly (Figure 1b), suggesting that the spirocyclic ring-opening of CR-Ac

as a result of  $\text{Cu}^{2+}$  binding. Meanwhile, an isosbestic point was observed at 448 nm, indicating the cleanly conversion of the free sensor into its  $\text{Cu}^{2+}$ -complex. The immediate and dramatic change in colour from yellow to greenish-blue allows a “naked-eye” detection of  $\text{Cu}^{2+}$  (Figure 1a inset).



**Scheme 1.** Synthesis of CR-Ac

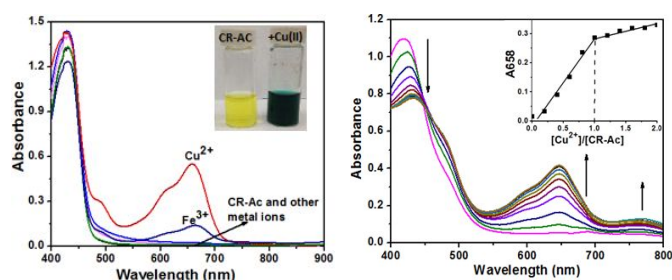


**Figure 1.** (a) Absorption responses of 20  $\mu\text{M}$  CR-Ac to various metal ions (20  $\mu\text{M}$  for  $\text{Cu}^{2+}$ ,  $\text{Ni}^{2+}$ ,  $\text{Mn}^{2+}$ ,  $\text{Hg}^{2+}$ ,  $\text{Zn}^{2+}$ ,  $\text{Ag}^+$ ,  $\text{Mg}^{2+}$ ,  $\text{Pb}^{2+}$ ,  $\text{Fe}^{3+}$ ,  $\text{Co}^{2+}$ ,  $\text{Fe}^{2+}$ ,  $\text{Cu}^+$  and  $\text{Cr}^{3+}$ ; 100  $\mu\text{M}$  for  $\text{Na}^+$ ,  $\text{K}^+$ ,  $\text{Mg}^{2+}$  and  $\text{Ca}^{2+}$ ) in ACN/MOPS buffer (10 mM, pH 7.04, v/v 1:1). (b) UV-vis spectra of CR-Ac with the addition of various concentrations of  $\text{CuCl}_2$  in ACN/MOPS buffer (10 mM, pH 7.04).

To examine the fluorescent response to  $\text{Cu}^{2+}$ , a solution of CR-Ac in ACN/MOPS buffer (10 mM, pH 7.04, v/v 1:1) was titrated with various concentrations of  $\text{Cu}^{2+}$  and monitored with a fluorometer by excitation at 425 or 650 nm, individually. When excited at 650 nm, CR-Ac itself is non-fluorescent ( $\phi_F = 0.02$ ). When  $\text{Cu}^{2+}$  was added to the CR-Ac solution, it displayed an emission peak with the maximum at 696 nm ( $\phi_F = 0.24$ ) (Figure 2a). When it was excited at 425 nm, the CR-Ac solution displayed one strong emission peak at 473 nm and a very weak one at 696 nm (Figure 2b). Upon  $\text{Cu}^{2+}$  was added to CR-Ac solution, a significant decrease in intensity of the 473 nm peak which gradually shifted to 520 nm and a marked concomitantly increase in intensity of the emission peak at 696 nm were observed (Figure 2b). The quenching of the ~473-520 nm emission can be attributed to the binding of the paramagnetic  $\text{Cu}^{2+}$  moiety while the “turn-on” to the 696 nm emission is due to the coordination-induced ring-opening of the spirocyclic moiety<sup>3d</sup>. These  $\text{Cu}^{2+}$ -induced spectral features on CR-Ac laid the foundation for  $\text{Cu}^{2+}$  detection and its concentration measurement via ratiometric fluorescent techniques.

We next tested the changes in fluorescence properties of CR-Ac as a result of the addition of various metal ions including  $\text{Cu}^{2+}$ ,  $\text{Ni}^{2+}$ ,  $\text{Mn}^{2+}$ ,  $\text{Hg}^{2+}$ ,  $\text{Na}^+$ ,  $\text{Ca}^{2+}$ ,  $\text{Zn}^{2+}$ ,  $\text{Ag}^+$ ,  $\text{Mg}^{2+}$ ,  $\text{Pb}^{2+}$ ,  $\text{K}^+$ ,  $\text{Fe}^{3+}$ ,  $\text{Co}^{2+}$ ,  $\text{Fe}^{2+}$ ,  $\text{Cu}^+$  and  $\text{Cr}^{3+}$ . As shown in Figure S1, significant 696 nm fluorescence “turn-on” (excitation at 650 nm) was only induced by  $\text{Cu}^{2+}$  (>65-fold enhancement with 1 eq. of  $\text{Cu}^{2+}$ ) with  $\text{Fe}^{3+}$  showing very minor response. The presence of any of the other metal ions tested (Figure 3a) does not affect the fluorescent intensity of CR-Ac with  $\text{Cu}^{2+}$ , suggesting little interferences from the other metal ions. We also examined the

ratiometric fluorescence response ( $F_{650}/F_{520}$ ) of CR-Ac to determine its selectivity to metal ions. As shown in Figure 3a, the solution of CR-Ac exhibits a very low fluorescent ratiometric value ( $F_{650}/F_{520}$ ) and it remains very low in the presence of the various metal ions (gray bars); but upon the addition of 1 equiv. of  $\text{Cu}^{2+}$ , there is a strong enhancement of this value, even in the presence of other metal ions tested (black bars). These data demonstrate that CR-Ac is highly selective to  $\text{Cu}^{2+}$  and the fluorescence response is not influenced by the other metal ions.

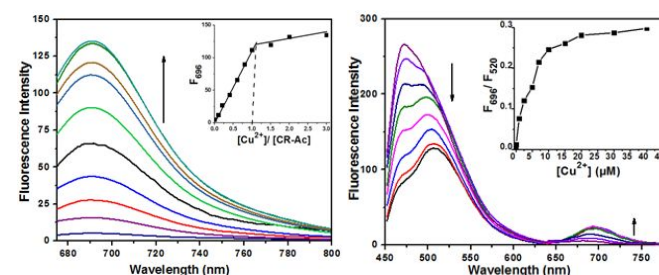


**Figure 2.** (a) Fluorescence response of 20  $\mu\text{M}$  CR-Ac to increasing concentration of  $\text{Cu}^{2+}$  (bottom to top, 0.0, 0.05, 0.1, 0.15, 0.2, 0.3, 0.5, 0.7, 0.8, 0.9, 1.0, 1.5 and 2.0 eq. in ACN/MOPS buffer (10 mM, pH 7.04, v/v 1:1), ( $\lambda_{\text{ex}}$  650 nm). (b) Fluorescence response of 20  $\mu\text{M}$  CR-Ac to increasing concentration of  $\text{Cu}^{2+}$  in ACN/MOPS buffer (10 mM, pH 7.04, v/v 1:1) ( $\lambda_{\text{ex}}$  420 nm)

Moreover, the effects of pH on the stability of the probe and its  $\text{Cu}^{2+}$ -complex were investigated and monitored by both absorption and fluorescent spectroscopies (Figure 3b and Figure S2). In contrast to the dramatic pH-dependent profile of the ACCu2-copper complex<sup>9</sup>, we found that the spectra of our probe CR-Ac and its  $\text{Cu}^{2+}$ -complex are both nicely stable over the biologically relevant pH range 5-9, which is key to its biological application. The fluorescence goes up a bit at low or high pH.

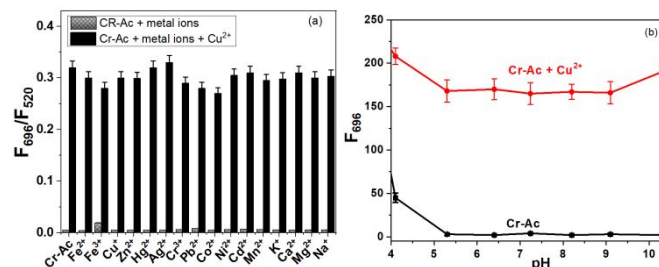


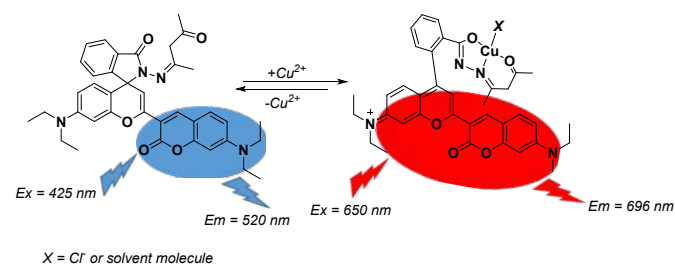
**Figure 3.** (a) Fluorescent responses  $F_{696}/F_{520}$  of 20  $\mu\text{M}$  CR-Ac to the presence of various metal ions (gray bars) and the subsequent addition of  $\text{Cu}^{2+}$  (black bar) in ACN/MOPS buffer (10 mM, pH 7.04, v/v 1:1). (b)

Variation of fluorescent response (696 nm) of CR-Ac and CR-Ac + Cu<sup>2+</sup> (20 μM each) at various pH values in ACN/H<sub>2</sub>O (1/1, v/v) solution.

The binding stoichiometry of CR-Ac and Cu<sup>2+</sup> was investigated by UV-vis titration which gives a 1:1 ratio (see Figure 1b inset) and was confirmed by Job's plot (Figure S3). The binding constant was calculated following a method reported previously<sup>11</sup>, using absorption values at 650 nm, and was determined to be  $1.92 \times 10^7 \text{ M}^{-1}$  (log K = 7.28) which is over 2 orders of magnitude higher than that of Cu<sup>2+</sup> to ACCu<sup>2+</sup>. Moreover, the fluorescent ratiometric change ( $F_{696}/F_{520}$ ) was linearly dependent on the concentration of Cu<sup>2+</sup> over the range from 0 to 10 μM ( $R^2 = 0.997$ ). The fluorescent detection limit in solution was determined to be 0.20 μM (based on  $3\sigma/k$ , Figure S4) which is 4 times lower than that of the ACCu<sup>2+</sup> sensor<sup>9</sup>

Reversibility is also key to monitoring the dynamics of Cu<sup>2+</sup> levels in intracellular store. The addition of metal chelator EDTA (5.0 eq.)

to the solution of CR-Ac-Cu<sup>2+</sup> caused the disappearance of the absorption signals of CR-Ac-Cu<sup>2+</sup> (Figure S5), suggesting that the Cu<sup>2+</sup>-binding process is reversible. The possible structures of this reversible binding process are shown in Scheme 2.



**Scheme 2.** The proposed reversible 1:1 binding mode between CR-Ac and Cu<sup>2+</sup> (X represents a possible ligand from the solvent)

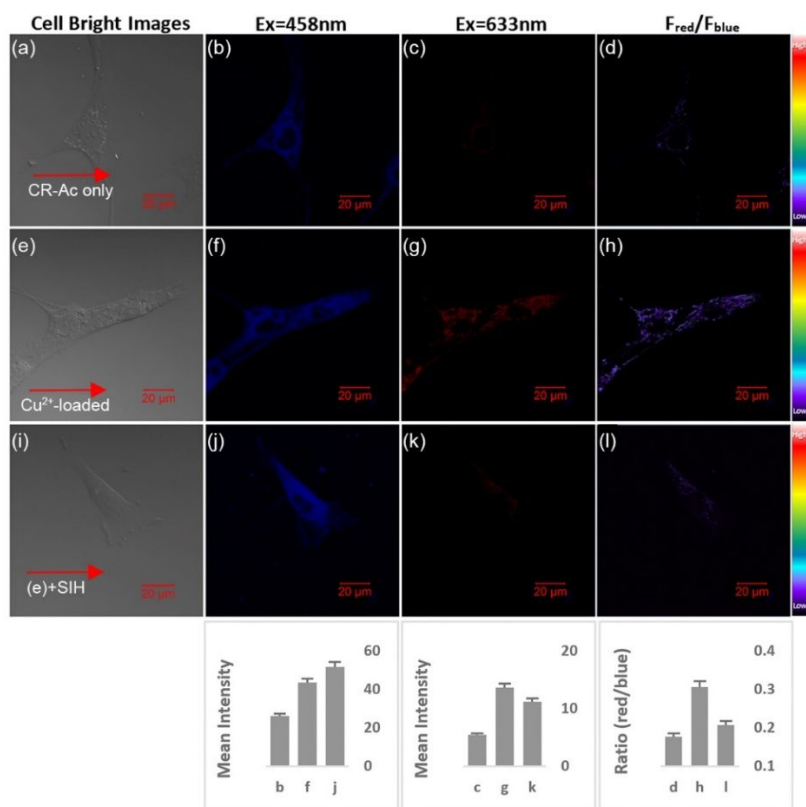


**Figure 4.** Confocal microscopy images (with DIC) of fibroblast cells (ws1) treated with (b,c) 10 μM CR-Ac sensor after 30 min incubation; (f,g) the cells were preincubated with Cu<sup>2+</sup> (20 μM) for 1 h before incubation with the sensor for 30 min; (j,k) the Cu<sup>2+</sup>-loaded cells were incubation with 100 μM chelator SIH for 7 h. Excitation wavelength was 458 nm for the blue channel (b,f,j) and 633 nm for the red channel (c,g,k). (d,h,l) are ratio images of c/b, g/f, k/j, respectively. The fluorescent intensities are shown in the bar chart at the bottom (n =6). Confocal ratiometric images are the average ratio in regions of interest.

Encouraged by the above promising results, we next tested the usefulness of the sensor CR-Ac in detecting Cu<sup>2+</sup> ions in living cells. Primary human fibroblast cells (ws1) were treated with 10–400 μM CR-Ac for 30–60 min at 37 °C and cell viability was monitored by confocal microscopy with Hoechst 33258 staining<sup>4d</sup>. Little cell death was observed even at 400 μM CR-Ac, suggesting negligible cytotoxicity. The cells exhibited a strong fluorescence in the blue channel (Figure 4b), indicating that the sensor CR-Ac is cell permeable. However, barely any fluorescent signals were detected in the red channel (Figure. 4c), presumably due to the very low basal level of free Cu<sup>2+</sup> in cells

<sup>1,13</sup>. When the cells were preloaded with Cu<sup>2+</sup> (20 μM) for 1 h, and then incubated with CR-Ac (10 μM) for 30 min, a marked enhancement in the red emission (Figure 4g and bar chart) was observed, matching those Cu<sup>2+</sup>-induced fluorescence changes (Figure 2), suggesting detectable level of free Cu<sup>2+</sup> in the cells. When the Cu<sup>2+</sup>-loaded cells were incubated with salicylaldehyde isonicotinoyl hydrazone (SIH, 100 μM), a membrane-permeable metal ion chelator that effectively removes Cu<sup>2+</sup> from cells<sup>12</sup>, a marked decrease in the red emission (Figure 4k and bar chart) and an increase in the blue emission (Figure 4j and bar chart) were observed, indicating a



significant reduction in cellular free  $\text{Cu}^{2+}$  level and that the binding of CR-Ac to  $\text{Cu}^{2+}$  is readily reversible in live-cells. Thus, CR-Ac exhibits facile fluorescent responses to  $\text{Cu}^{2+}$  ions in living cells and is capable of imaging the presence of  $\text{Cu}^{2+}$  ions as well as its dynamic changes in cells.

The dynamic changes of free  $\text{Cu}^{2+}$  levels in the  $\text{Cu}^{2+}$ -loaded cells and SIH-treated cells are also readily revealed by ratiometric imaging (Figure 4d,h,i and bar chart).

To quantify free  $\text{Cu}^{2+}$  levels in cells, *in situ* cell calibrations<sup>12</sup> were performed via ratiometric imaging using pyriothione as a  $\text{Cu}^{2+}$  ionophore<sup>5c</sup> in FBS-free media. The calibration curve gives a linear response to cellular free  $[\text{Cu}^{2+}]$  up to 400 nM with an *in situ* detection limit *ca.* 7 nM (Figure S6). Evident cell death at higher  $[\text{Cu}^{2+}]$ , presumably due to copper toxicity, prevents meaningful  $[\text{Cu}^{2+}]$  analysis. Analysis of the ratiometric images in Figure 4 gives free  $[\text{Cu}^{2+}]$  262 nM in  $\text{Cu}^{2+}$ -loaded ws1 cells (Figure 4h) and 89 nM in the subsequently SIH-treated cells (Figure 4i). The free  $[\text{Cu}^{2+}]$  in untreated ws1 cells (Figure 4d) is below the detection limit of the sensor. This is reasonable because free copper ions are known to be very low in cells<sup>1,5c,14</sup>. The nanomolar level of free  $\text{Cu}^{2+}$  in ws1 cells after  $\text{Cu}^{2+}$ -loading is lower than those in a previous report<sup>9</sup> which *in situ* cell calibration was not used for  $[\text{Cu}^{2+}]$  determination and different cell lines were used.

The images of the  $\text{Cu}^{2+}$ -loaded cells from the red and ratiometric channels showed scattered patterns, implying that  $\text{Cu}^{2+}$  in the cells (ws1) may be localized in certain subcellular compartments (organelles) and that CR-Ac may be capable of imaging  $\text{Cu}^{2+}$  ions at subcellular resolution. The subcellular distribution of  $\text{Cu}^{2+}$  ions in the cells was further investigated by colocalization experiments using organelle dyes—MitoTracker Green FM and LysoTracker Blue DND-99<sup>4d</sup>. As illustrated in Figure S7, no colocalization between the  $\text{Cu}^{2+}$ -induced fluorescence (red) and LysoTracker blue images was observed, suggesting that the detected free  $\text{Cu}^{2+}$  is not located in lysosomes. In contrast, a complete colocalization between the red fluorescence and the Mito-tracker green signals was observed (Figure S8), indicating that the detected  $\text{Cu}^{2+}$  ions are located in mitochondria of ws1 cells. This mitochondria location of the  $\text{Cu}^{2+}$  pool is reasonable as it is where  $\text{Cu}^{2+}$  is needed in cells for Cu-relying enzymes such as cytochrome c oxidase.<sup>1</sup>

Collectively, the results show excellent sensor characteristics of CR-Ac in reporting the dynamic changes in cytoplasmic labile  $\text{Cu}^{2+}$  at subcellular resolution as well as concentration estimation at nanomolar level. The one-photon, turn-on, ratiometric and NIR photo properties, high solubility in culture medium and selectivity, reversible response, resistant to pH change and fast response time make it an excellent tool to study the cell biology of copper as well as its related diseases.

We thank the National Science Foundation (CHE-1213838, CHE-1229339) and NIH (1R15GM126576-01) for funding.

## Conflicts of interest

The conflicts of interest issue is being processed by the OTCV office of University of Massachusetts Dartmouth.

## Notes and references

- a) D. G. Barceloux, D. Barceloux, *Clin. Toxicol.*, 1999, **37**, 217; b) N. J. Robinson, D. R. Winge, *Annu. Rev. Biochem.* 2010, **79**, 537; c) H. Tapiero, D. M. Townsend, K. D. Tew, *Biomed Pharmacother.* 2003, **57**, 386; d) E. Gaggelli, H. Kozlowski, D. Valensin, G. Valensin, *Chem. Rev.* 2006, **106**, 1995. e) P. Verwilst, K. Sunwoo, J. S. Kim, *Chem. Commun.* 2015, **51**, 5556.
- a) D. J. Waggoner, T. B. Bartnikas, J. D. Gitlin, *Neurobiol. Disease*, 1999, **6**, 221; b) K. J. Barnham, C. L. Masters, A. I. Bush, *Nat. Rev. Drug Discov.* 2004, **3**, 205.
- a) C. A. Flemming, J. T. Trevors, *Water Air Soil Pollut.*, 1989, **44**, 143; b) L. Li, D. Pan, B. Li, Y. Wu, H. Wang, Y. Gu, T. Zuo, *Resour. Conserv. Recy.*, 2017, **127**, 1.
- a) E. Que, D.W. Domaille, C.J. Chang, *Chem. Rev.* 2008, **108**, 1517; b) X. Chen, T. Pradhan, F. Wang, J.S. Kim, Y. Yoon, *Chem. Rev.*, 2012, **112**, 1910; c) K. P. Carter, A. M. Young, A. E. Palmer, *Chem. Rev.* 2014, **114**, 4564; d) Y. Wei, Z. Aydin, Y. Zhang, Z. Liu, M. Guo, *ChemBiochem*, 2012, **13**, 1569; e) S. Maiti, Z. Aydin, Y. Zhang, M. Guo, *Dalton Trans.* 2015, **44**, 8942.
- a) G. Sivaraman, M. Iniya, T. Anand, N.G. Kotla, O. Sunnapu, S. Singaravadivel, A. Gulyani, D. Chellappa, *Coord. Chem. Rev.* 2018, **357**, 50; b) C. Yin, J. Li, F. Hou, *Curr. Med. Chem.* 2019, **26**, 3958; c) B. J. McCranor, H. Szmanski, H. H. Zeng, A. K. Stoddard, T. Hurst, C. A. Fierke, J. R. Lakowicz and R. B. Thompson, *Metallomics*, 2014, **6**, 1034; d) Y. Ha, D. P. Murale, S. T. Manjare, M. Kim, J. A. Jeong, D. G. Churchill, *Bull. Korean Chem. Soc.* 2016, **37**, 69.
- a) L. Hou, X. Kong, Y. Wang, J. Chao, C. Li, C. Dong, Y. Wang, S., *J. Mater. Chem. B*, 2017, **5**, 8957; b) K. Liu, S. Xu, P. Guo, L. Liu, X. Shi, B. Zhu, *Anal. Bioanal. Chem.* 2019, 411, 3021.
- a) A. Lee, J. Chin, O. K. Park, H. Chung, J. W. Kim, S. Y. Yoon, K. Park, *Chem. Commun.* 2013, **49**, 5969; b) R. Guo, Q. Wang, W. Lin, *J. Fluoresc.* 2017, **27**, 1655; c) X. Wang, P. Xia, X. Huang, *Spectrochim. Acta - Part A Mol. Biomol. Spectrosc.*, 2019, **210**, 98.
- a) Y. Chen, C. Zhu, J. Cen, J. Li, W. He, Y. Jiao, Z. Guo, *Chem. Commun.* 2013, **49**, 7632; b) Y. Fu, C. Ding, A. Zhu, Z. Deng, Y. Tian, M. Jin, *Anal. Chem.* 2013, **85**, 11936; c) S. Y. Park, W. Kim, S. H. Park, J. Han, J. Lee, C. Kang, M. H. Lee, *Chem. Commun.* 2017, **53**, 4457; d) L. Yang, M. Zeng, Y. Du, L. Wang, B. Peng, *Luminesc.* 2018, **33**, 1268.
- D. E. Kang, C. S. Lim, J. Y. Kim, E. S. Kim, H. J. Chun, B. R. Cho, *Anal. Chem.* 2014, **86**, 5353.
- a) D. Cao, Z. Liu, P. Verwilst, S. Koo, P. Jangjili, J. S. Kim, W. Lin, *Chem. Rev.* 2019, **119**, 10403; b) J. Liu, Y. Q. Sun, P. Wang, J. Zhang and W. Guo, *Analyst*, 2013, **138**, 2654
- a) M. Guo, C. A. Perez, Y. Wei, E. Rapoza, G. Su, F. B. Abdallah, N. D. Chasteen, *Dalton Trans.*, 2007, 4951; b) C. Perez, M. Guo, *J. Inorg. Biochem* 2009, **103**, 326.
- a) J. L. Buss, E. Arduini, K. C. Shephard, P. Ponka, *Biochem. Pharmacol.* 2003, **65**, 349; b) Y. Wei, Y. Zhang, Z. Liu, M. Guo *Chem. Commun.* 2010, **46**, 4472
- G. Rong, E. H. Kim, K. E. Poskanzer, H. A. Clark, *Sci. Rep.* 2017, **7**, 10819 | DOI:10.1038/s41598-017-11162-8
- a) P. C. Bull, G. R. Thomas, J. M. Rommens, J. R. Forbes, D. W. Cox, *Nat. Genet.* 1993, **5**, 327; b) T. D. Rae, P. J. Schmidt, R. A. Pufahl, V. C. Culotta, T. V. O'Halloran, *Science* 1999, **284**, 805.